

# PHYSICAL REVIEW B

## CONDENSED MATTER AND MATERIALS PHYSICS

THIRD SERIES, VOLUME 61, NUMBER 6

1 FEBRUARY 2000-II

### RAPID COMMUNICATIONS

*Rapid Communications are intended for the accelerated publication of important new results and are therefore given priority treatment both in the editorial office and in production. A Rapid Communication in Physical Review B may be no longer than four printed pages and must be accompanied by an abstract. Page proofs are sent to authors.*

#### Deformation behavior of Zr-based bulk nanocrystalline amorphous alloys

Cang Fan, Chunfei Li, and Akihisa Inoue\*

*Japan Science and Technology Corporation, Sendai 982-0807, Japan*

Volker Haas

*Institute for Solid State and Materials Research Dresden, Helmholtzstrasse 20, 01169 Dresden, Germany*

(Received 9 August 1999; revised manuscript received 2 December 1999)

Mechanical properties of bulk  $Zr_{55}Ni_5Cu_{30}Al_{10}$  metallic glass alloy and  $Zr_{53}Ti_5Ni_{10}Cu_{20}Al_{12}$  nanocrystalline-amorphous alloy were measured by compression tests at room temperature. Although no distinct plastic deformation is recognized in the  $Zr_{55}Ni_5Cu_{30}Al_{10}$  metallic glass, the  $Zr_{53}Ti_5Ni_{10}Cu_{20}Al_{12}$  as-quenched alloy exhibits significant plastic strain. Moreover, we found that both the strength and plastic strain increased significantly with increasing volume fraction of nanocrystals, and the plastic strain achieved a maximum in the early stage of nanocrystallization. High-resolution electron microscopy showed that nanocrystals with average grain sizes of about 2.0 and 2.5 nm were embedded in the amorphous matrix of the as-quenched bulk  $Zr_{53}Ti_5Ni_{10}Cu_{20}Al_{12}$  alloy and the specimen with the maximum plastic strain, respectively.

Melt-spun amorphous alloys are known to exhibit both high strength and good bending ductility. However, upon annealing-induced crystallization, both properties are generally lost.<sup>1</sup> For the last decade of this century, with the development of techniques making nanostructured materials, a substantial increase in the strength has been observed in a number of nanocrystalline-amorphous alloys prepared by isothermal annealing,<sup>2,3</sup> especially in several bulk nanocrystalline-amorphous alloys.<sup>4-7</sup>

However, with bulk nanocrystalline-amorphous alloys a decrease in ductility but with a concurrent increase in strength with increasing volume fraction of nanocrystals is observed.<sup>5</sup> This behavior was interpreted to be due to the supposed brittleness of the precipitated nanocrystals.

In the present work we investigated the mechanical properties measured by compression tests and the microstructures observed by optical and high-resolution electron microscopy in bulk  $Zr_{53}Ti_5Ni_{10}Cu_{20}Al_{12}$  nanocrystalline-amorphous alloy. In contrast to investigations reported hitherto, we found that the compressive plastic strain increased with increasing volume fraction of nanocrystals.

$Zr_{53}Ti_5Ni_{10}Cu_{20}Al_{12}$  ingots were initially prepared by arc melting the mixtures of pure metals in a purified argon at-

mosphere and cast into a copper mould in vacuum. The alloy crystallizes via precipitation of a metastable phase in the primary crystallization step leading to nanoparticles embedded in an amorphous matrix.<sup>7</sup> For comparison, a  $Zr_{55}Ni_5Cu_{30}Al_{10}$  amorphous alloy, which shows the typical large glass-forming ability,<sup>8</sup> was also prepared. X-ray measurements were performed on as-cast specimens to check the amorphicity of the sample. The amorphous alloys were partially crystallized by isothermal annealing in the supercooled liquid region, and the volume fraction  $V_f$  of nanocrystals was estimated by differential scanning calorimetry (DSC) (i.e.,  $V_f$  proportional to the heat release upon partial crystallization). Microstructures of the specimens were examined by high-resolution electron microscopy (HREM) (JEM-3000F, operated at 300 kV). The mechanical properties were measured by compression tests using cylinders of 2.0 mm in diameter and 4.5 mm long at a strain rate of  $4.4 \times 10^{-4} \text{ s}^{-1}$  at room temperature. Young's modulus was measured by a strain gauge. The shear bands of a sample strained to 0.6% compressive plastic strain were investigated by optical microscopy (OM).

Figure 1 shows the compressive stress-strain curves: (a) for bulk  $Zr_{55}Ni_5Cu_{30}Al_{10}$  amorphous alloy; (b), (c), and (d) for as-quenched and exemplarily for the investigated an-

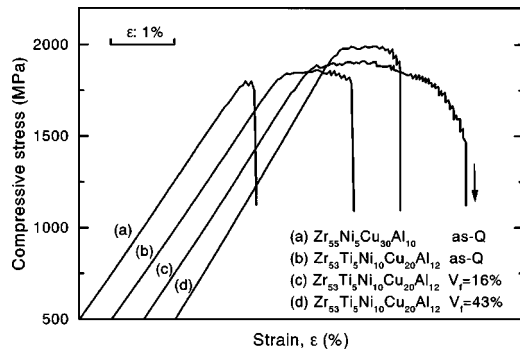


FIG. 1. Compressive stress-strain curves at room temperature: (a) for bulk  $Zr_{55}Ni_5Cu_{30}Al_{10}$  amorphous alloy; (b), (c), and (d) for as-quenched and nanocrystalline bulk  $Zr_{53}Ti_5Ni_{10}Cu_{20}Al_{12}$  alloys.

nealed bulk  $Zr_{53}Ti_5Ni_{10}Cu_{20}Al_{12}$  alloys. The stress-strain relation is linear up to about 1.8–2% compressive strain. Beyond this strain plastic deformation sets in as is evident by unloading the specimen. No distinct plastic deformation is observed in the  $Zr_{55}Ni_5Cu_{30}Al_{10}$  amorphous alloy, but the Ti containing the as-quenched alloy exhibits a plastic strain being several times that of  $Zr_{55}Ni_5Cu_{30}Al_{10}$ , the amorphous reference, indicating the improved ductility of the nanocrystal-forming alloy. Furthermore, in the partially crystallized  $Zr_{53}Ti_5Ni_{10}Cu_{20}Al_{12}$  alloy at  $V_f=16\%$ , the curve shows a further improved plastic strain being about two times as large as that of the corresponding as-quenched alloy. In addition, stress decreases considerably after reaching the maximum value. In the  $V_f=43\%$  sample, plastic strain is smaller than that of the as-quenched one but much larger than that of  $Zr_{55}Ni_5Cu_{30}Al_{10}$  the amorphous reference.

The mechanical properties of the  $Zr_{53}Ti_5Ni_{10}Cu_{20}Al_{12}$  alloy with different volume fractions of nanocrystals are shown in Table I. The plastic strain is 1.4% for the as-quenched one and increases with increasing  $V_f$ , reaching a maximum value of 2.5% at  $V_f=16\%$ . Upon further increasing  $V_f$ , the plastic strain starts to decrease again, but is still about 1.0% at  $V_f=43\%$ . While the measured strains are at variance with previous results,<sup>5</sup> the generally observed increase in Young's modulus, compressive yield strength, and the maximum strength was found in this nanocrystalline alloy as well.

In order to examine the reason of the increased ductility, we have also studied the microstructure of the specimen, which showed the maximum value of plastic strain, and an as-quenched one for comparison by HREM. Figure 2 shows

TABLE I. Mechanical properties of  $Zr_{53}Ti_5Ni_{10}Cu_{20}Al_{12}$  alloy with different volume fractions of nanocrystals.

Fraction of nanocrystals (vol %)	Yield strength (MPa)	Maximum strength (MPa)	Young's modulus (MPa)	Plastic strain (%)
0	1490	1760	81	1.4
10	1530	1770	82	2.2
16	1540	1810	92	2.5
28	1730	1890	95	1.5
43	1820	1950	106	1.0

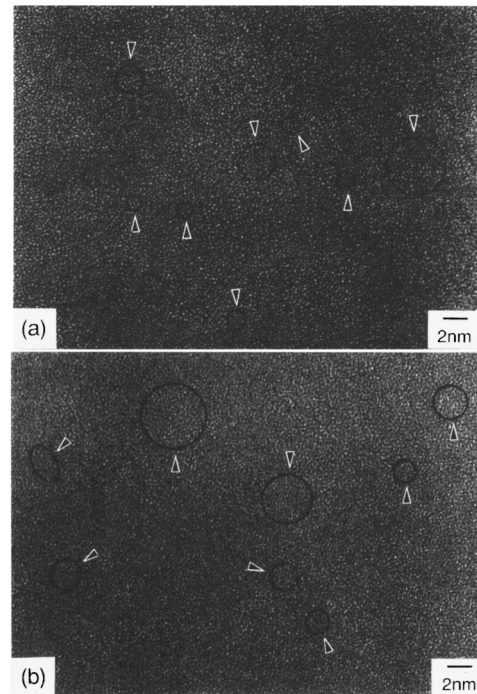


FIG. 2. High-resolution electron microscopy images of (a) the as-quenched specimen and (b) the annealed specimen with  $V_f=16\%$  of the bulk  $Zr_{53}Ti_5Ni_{10}Cu_{20}Al_{12}$  alloy. Nanocrystals are indicated by arrows.

the images of (a) the as-quenched specimen and (b) the annealed specimen with  $V_f$  of 16% of the bulk  $Zr_{53}Ti_5Ni_{10}Cu_{20}Al_{12}$  alloy. Although x-ray analysis and conventional transmission electron microscopy suggest the as-quenched specimen to be completely amorphous, HREM reveals many fine crystals (arrows in Fig. 2) dispersed in the amorphous matrix. The sizes range mainly from 1.5 to 2.5 nm and their average value is about 2 nm. The microstructure is different from the microstructure of the  $Zr_{55}Ni_5Cu_{30}Al_{10}$  alloys, which are purely amorphous. The micrograph of the  $V_f=16\%$  shows larger nanocrystals, which is a metastable compound phase<sup>7</sup> supposed to exhibit a large hardness and brittleness, with main grain sizes of about 2–3 nm (average grain size is about 2.5 nm, and the largest one less than 5 nm). In both cases the particles are spherical and almost no defects are observed within the particles. The crystal orientation of each particle appears to be completely randomly distributed as well.

Macroscopic information about the nature of the plastic deformation of the nanocrystalline-amorphous alloys was obtained by optical microscopy. Figure 3 shows the surface appearance of an annealed specimen with  $V_f=16\%$  strained to about 0.6% plastic strain. At the early stage of plastic deformation, many localized slip bands marked by arrows are observed and the angle of the slip bands to the compressive is approximately  $50^\circ$ . This is different from the one with a much larger  $V_f$  as well as  $Zr_{55}Ni_5Cu_{30}Al_{10}$  specimens, where only few slip bands are found even after fracture has occurred. This suggests that plastic flow takes place more homogeneously in  $Zr_{53}Ti_5Ni_{10}Cu_{20}Al_{12}$  specimens with  $V_f=16\%$ .

Currently, it does not seem properly understood what mechanisms are responsible for the hardening observed in

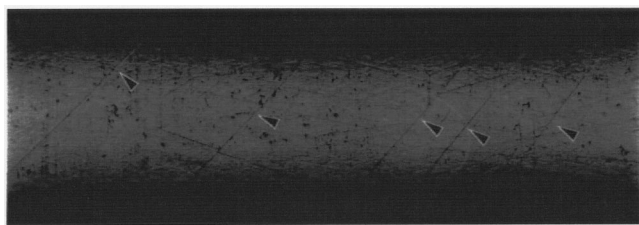


FIG. 3. The nature of the plastic deformation of the bulk  $Zr_{53}Ti_5Ni_{10}Cu_{20}Al_{12}$  nanocrystalline-amorphous alloy ( $V_f=16\%$ ) with about 0.6% of the plastic strain observed by an optical microscope ( $\times 10$ ). Localized shear bands are marked by arrows.

partially crystallized alloys. So far, the increase in strength and concurrent decrease in ductility in partially crystallized bulk nanocrystalline-amorphous alloys was attributed to the supposed hardness and brittleness of the nanocrystals.<sup>5</sup> Upon loading, they would not deform and act as obstacles preventing shear bands to move. Thus, the yield stress is raised while at the same time ductility decreases because the shear bands, in which plastic deformation takes place, cannot move freely through the material. While this argument may qualitatively explain the observed increase in strength, it fails to explain the increased ductility in our experiments.

However, our results may be explained if one makes an additional assumption. One could imagine that because of the stress concentration at a (nano-) crystal, shear bands are more easily nucleated in its vicinity. If this is the case the deformation behavior must strongly depend on the size, morphology, and spatial distribution of these nanocrystals. With  $Zr_{53}Ti_5Ni_{10}Cu_{20}Al_{12}$ , the nanocrystals are spherical and only 2.5 nm in size on average and, as seen in the HREM, they are homogeneously distributed. From such an arrangement one would expect that thin shear bands develop at *many* points in the material. Thus, the deformation might be restricted to occur within one shear band, but because there are many of them, macroscopically, deformation becomes more homogeneously distributed over the material and, thus, better ductility is achieved. Vice versa, the model could also explain the vanishing ductility observed with other partially crystallized

bulk amorphous alloys.<sup>9</sup> Here, very often the crystals are relatively few, dendritic in shape, or large ( $\mu\text{m}$  range). Hence, shear bands could form only at few sites within the material. Thus, also macroscopically, deformation is inhomogeneous because it would be restricted to the few shear bands and no ductility is measured.

So far we have only discussed the behavior at the early stages of crystallization. At higher volume fractions of nanocrystals a change in the behavior occurs. Consistent with the observations of Leonhard *et al.*<sup>9</sup> the maximum tensile strength increases while ductility decreases again. From the above argument one would expect that with increasing  $V_f$  deformation becomes macroscopically more and more homogeneous because more and more shear bands should be formed. However, with increasing  $V_f$  the grain size becomes larger and more brittle. In addition, the distance between nanocrystals becomes very small, making it difficult for the shear band to move through the material. Thus, plastic deformation becomes restricted to the few shear bands that can move. This in turn renders deformation more inhomogeneous, and macroscopically we observe a decrease in ductility. This argument is supported by our OM observations. With increasing  $V_f$  one should see more shear bands, but in fact, there are less. Hence, deformation becomes more concentrated again on a few shear bands or, in other words, more inhomogeneous.

In conclusion, the existence of nanocrystals only a few nanometers in diameter and dispersed in an amorphous matrix was found to lead to an increase of both the strength and the ductility with increasing  $V_f$  of nanocrystals in early stages of the nanocrystallization in  $Zr_{53}Ti_5Ni_{10}Cu_{20}Al_{12}$ . The increased ductility was explained by the multiplication of shear bands due to the stress concentration in the vicinity of the nanocrystals. This multiplication is suggested to lead to a macroscopically more homogeneous deformation and, thus, to an increase of ductility.

C. Fan would like to thank Dr. Zheng Tang at the Institute for Materials Research of Tohoku University, Sendai, Japan, for useful discussions.

\*Also at Institute for Materials Research, Tohoku University, Sendai 980-8577, Japan.

<sup>1</sup>H. S. Chen, Rep. Prog. Phys. **43**, 353 (1980).

<sup>2</sup>Y. H. Kim, A. Inoue, and T. Masumoto, Mater. Trans., JIM **31**, 747 (1990).

<sup>3</sup>S. G. Kim, A. Inoue, and T. Masumoto, Mater. Trans., JIM **32**, 875 (1991).

<sup>4</sup>C. Fan, A. Takeuchi, and A. Inoue, Mater. Trans., JIM **40**, 42 (1999).

<sup>5</sup>L. Q. Xing, J. Eckert, W. Loser, and L. Schultz, Appl. Phys. Lett. **74**, 664 (1999).

<sup>6</sup>R. Busch, S. Schneider, A. Peker, and W. L. Johnson, Appl. Phys. Lett. **67**, 1544 (1995).

<sup>7</sup>C. Fan, D. V. Louzguine, C. Li, and A. Inoue, Appl. Phys. Lett. **75**, 340 (1999).

<sup>8</sup>A. Inoue and T. Zhang, Mater. Trans., JIM **37**, 185 (1996).

<sup>9</sup>A. Leonhard, L. Q. Xing, M. Heilsdaier, A. Gebert, J. Eckert, and L. Schultz, Nanostruct. Mater. **10**, 805 (1998).